SPACE TELESCOPE SCIENCE INSTITUTE
Operated for NASA by AURA

HLA Instrument Science Report 2008-01

ACS CCD Image Anomalies in the Hubble Legacy Archive

M. Stankiewicz[1], S. Gonzaga, B. Whitmore
Dec 5, 2008

ABSTRACT

The Hubble Legacy Archive (HLA) was created to make high-quality calibrated HST image products easily available to the astronomy research community. In its first public release, the HLA database has been populated with calibrated images from the Advanced Camera for Surveys (ACS). This report serves as a guide to identify ACS image anomalies that cannot currently be corrected in the HLA calibration pipeline.

Introduction

The Hubble Legacy Archive is an enhanced archive interface for browsing and retrieving images from the Hubble Space Telescope. It is designed primarily for research scientists, but is accessible to the public at large. The HLA is a joint project of the Space Telescope Science Institute, the European Coordinating Facility, and the Canadian Astronomy Data Centre.

The primary enhancements include:

1. Putting the data online for immediate access.
2. Adding a footprint service to make it easier to browse and download images.
3. Providing more extensive "composite images" (e.g., stacked, color, mosaics).
4. Improving absolute astrometry (i.e., from ~1-2" to ~0.3") when there is sufficient overlap with the Guide Star Catalog 2 (GSC2)
5. Developing source lists using SExtractor and DAOfind (in progress)
6. NICMOS grism extractions (produced at ECF)

[1] STScI & Parkville High School, Baltimore, Maryland.

Images in the HLA database are processed using standard pipeline calibration settings. In the first calibration phase, bias, dark, and flat-field corrections are applied to the images using the STSDAS task *calacs*. The images are then processed by Multidrizzle for geometric distortion corrections and image combination based on information in the association tables.

In October 2007, the HLA was in the Early Data Release phase of the project, populated with about 25% of all ACS data. A formal Data Release is planned for January 2008. Future enhancements include a completed ACS image database, as well as the addition of WFPC2, STIS, and eventually NICMOS data.

Analysis

During the summer of 2007, as the HLA database was being populated with ACS WFC and HRC images, systematic visual data quality checks were done on all image products. Suspicious cases were set aside for detailed inspection. Some were due to problems with the processing (e.g. data dropouts), while other anomalies were inherent to the images and could not be easily fixed. This ISR is designed to help you recognize and interpret both types of anomalies. If you encounter any data processing anomalies that have not been fixed in the HLA, please send a note to *archive@stsci.edu* and we will attempt to reprocess the data.

1.0 Hardware-related Anomalies

1.1 Background Quadrant Mismatch in ACS/WFC Images

WFC images are read out using four amplifiers, two for each detector. Because each amplifier has a specific bias level and structure, each quadrant is treated independently in the calibration process. The bias level subtracted from each image quadrant is derived from the last 6 columns of the physical overscan adjacent to the active imaging area. Ideally, for each quadrant, the offset between the overscan and active image areas should be constant. But in practice, small random differences occur in the offsets, on the order of a few tenths of a DN. These variations are probably caused by interference between the WFC integrated electronics module and the telescope and/or other science instruments. Point source photometry using local background subtraction is not impacted by this anomaly, unless the object falls on a quadrant border. But the surface photometry of extended objects across quadrants are affected by this problem.

Additional Information:

Bias Subtraction and Correction of ACS/WFC Frames

http://www.stsci.edu/hst/HST_overview/documents/calworkshop/workshop2002/CW2002_Papers/CW02_sirianni

ACS Data Handbook, Section 5.2,1, Bias Calibration Issues

http://www.stsci.edu/hst/acs/documents/handbooks/DataHandbookv5/ACS_longdhb.pdf

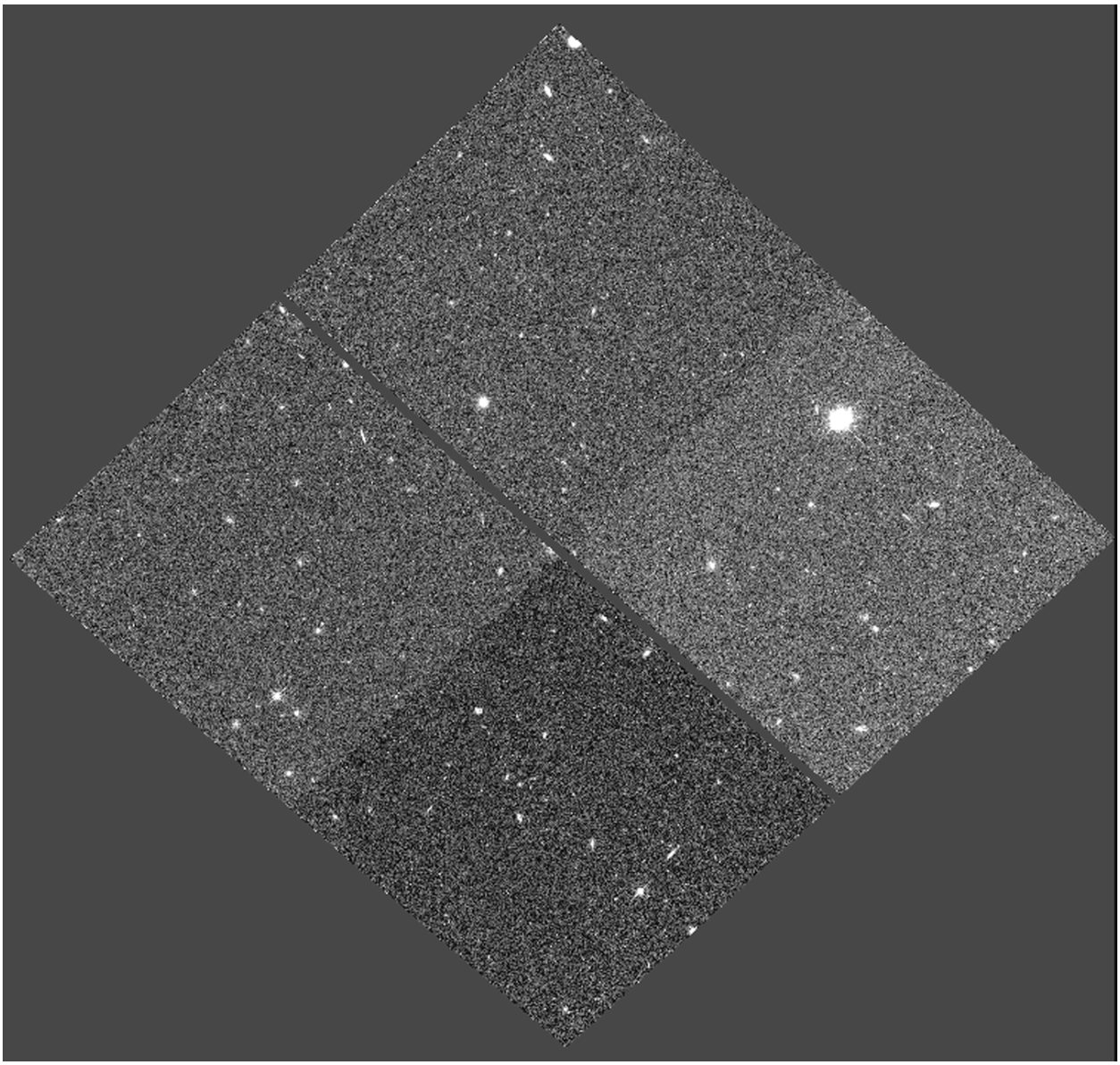

Figure 1.1 Image HST_9575_as_ACS_WFC_F625W, stretched to show the small bias level mismatches between quadrants.

1.2 Severe CCD Charge Bleeding

The full-well capacity for the CCDs in the WFC is 84,700 e^-, with variations of about 10% across the chips. For the HRC, that value is 155,000 $e^-$with an 18% variation. When the CCD pixels are over-exposed to a bright object, the full-well capacity is filled, causing charge to overflow into the immediate neighboring pixels along the column.

Additional Information:

ACS Instrument Handbook, Section 4.3.1, CCD Saturation: the CCD Full Well
http://www.stsci.edu/hst/acs/documents/handbooks/cycle16/acs_ihb.pdf

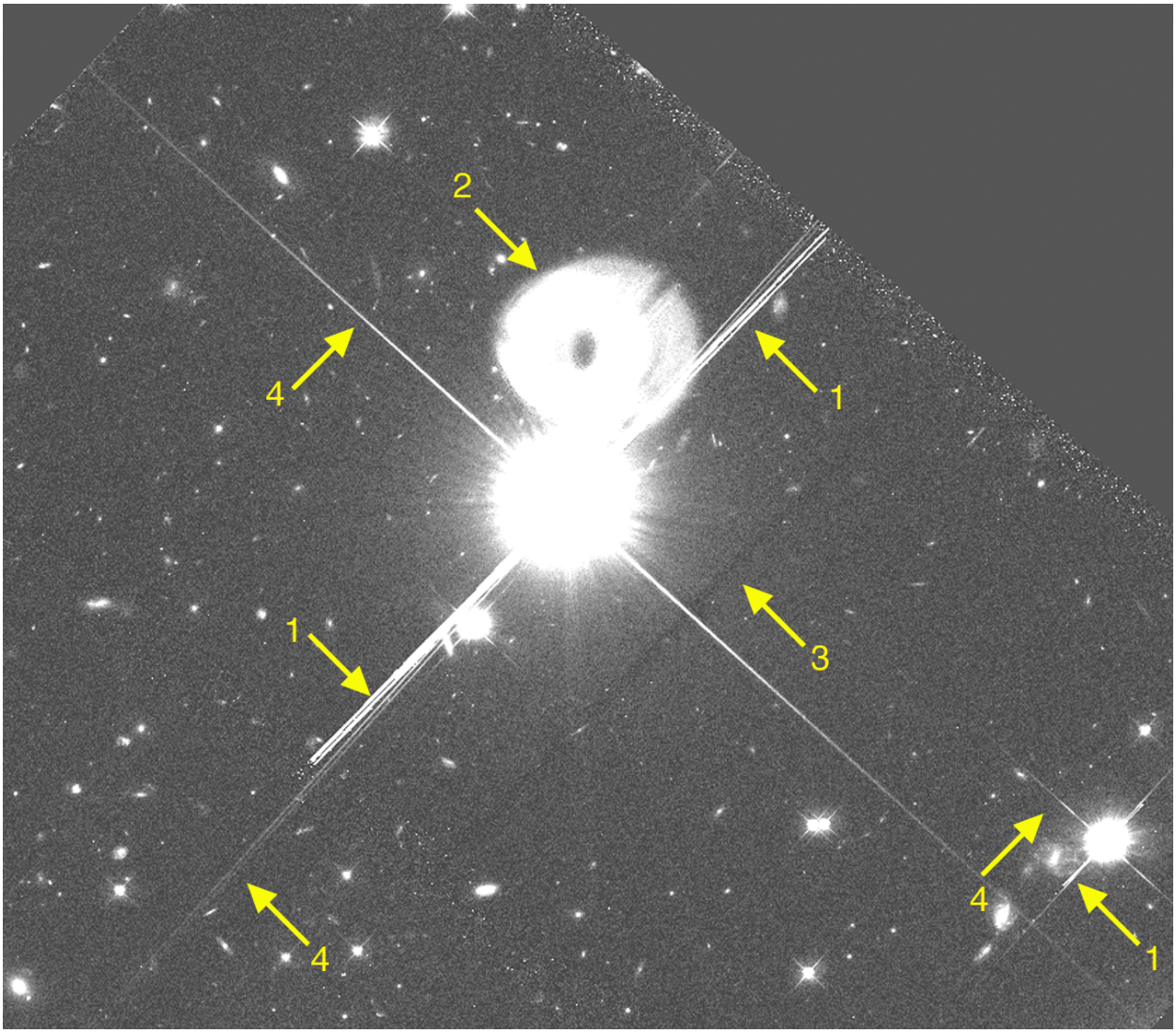

Figure 1.2 HST_10420_06_ACS_WFC_F606W_drz.fits shows: (1) Charge bleeding across the columns of bright stars, (2) a large annular feature due to internal optical reflections, (3) a dark band created by cross-talk, covered in Section 1.4, and (4) diffraction spikes.

1.3 Bad Columns

Some bad columns are permanent defects in the CCD, and are recorded in the data quality file, extension [2], in the FITS file. These bad columns can be removed from a combined image if its individual exposures are dithered (small spatial offsets between exposures). But if individual images were not dithered, the bad columns cannot be removed from the combined image.

Additional Information:

ACS data quality flags

http://www.stsci.edu/hst/acs/analysis/reference_files/data_quality_flags.html

ACS Instrument Handbook, Table 3.4, Flags for the DQ array

http://www.stsci.edu/hst/acs/documents/handbooks/cycle16/acs_ihb.pdf

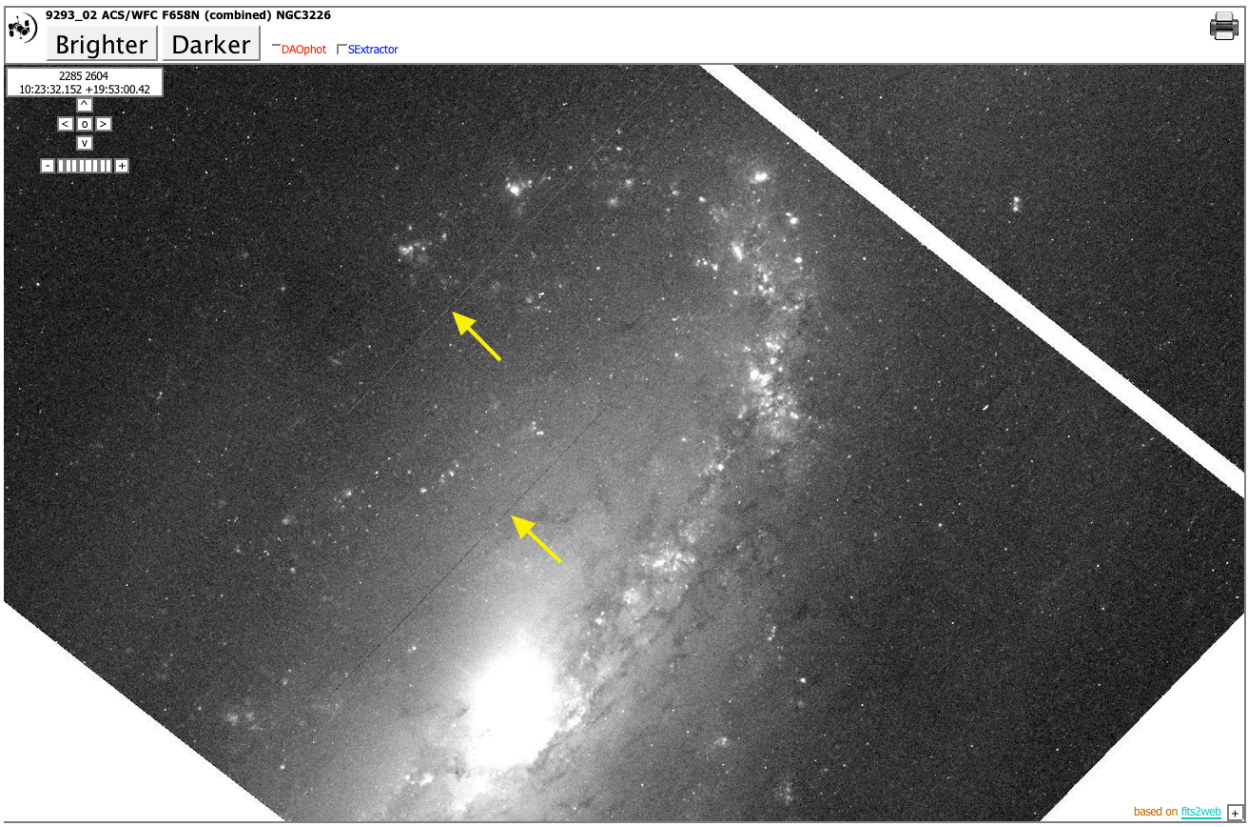

Figure 1.3 Section of image 9293_02 ACS/WFC F658N (combined) NGC3226 was created from two undithered images with the same bad columns, so those columns appear in the final combined image.

1.4 Cross-talk

Cross-talk among the four amplifiers in the WFC can produce faint ghost images of relatively bright sources. Positions of these ghosts are mirror-symmetric on other quadrants, relative to the originating source. Count rates for cross-talk features are typically 1 to 4 DN/pixel below background level. However, faint positive ghosts have also been seen. The impact on data analysis is minor since the ghosts, usually affecting very few pixels, have a small effect on total counts.

Additional Information:

ACS Data Handbook, Section 5.5.3 Cross Talk
http://www.stsci.edu/hst/acs/documents/handbooks/DataHandbookv4/ACS_longdhb.pdf

CCD amplifier cross-talk, or electronic ghosts
http://www.stsci.edu/hst/acs/performance/anomalies/zoo_xtalk.html

Cross-Talk in the ACS WFC Detectors. I: Description of the Effect (ISR 04-12)
http://www.stsci.edu/hst/acs/documents/isrs/isr0412.pdf

Cross-Talk in ACS WFC Detectors. II: Using GAIN=2 to Minimize the Effect (ISR 04-13)
http://www.stsci.edu/hst/acs/documents/isrs/isr0413.pdf

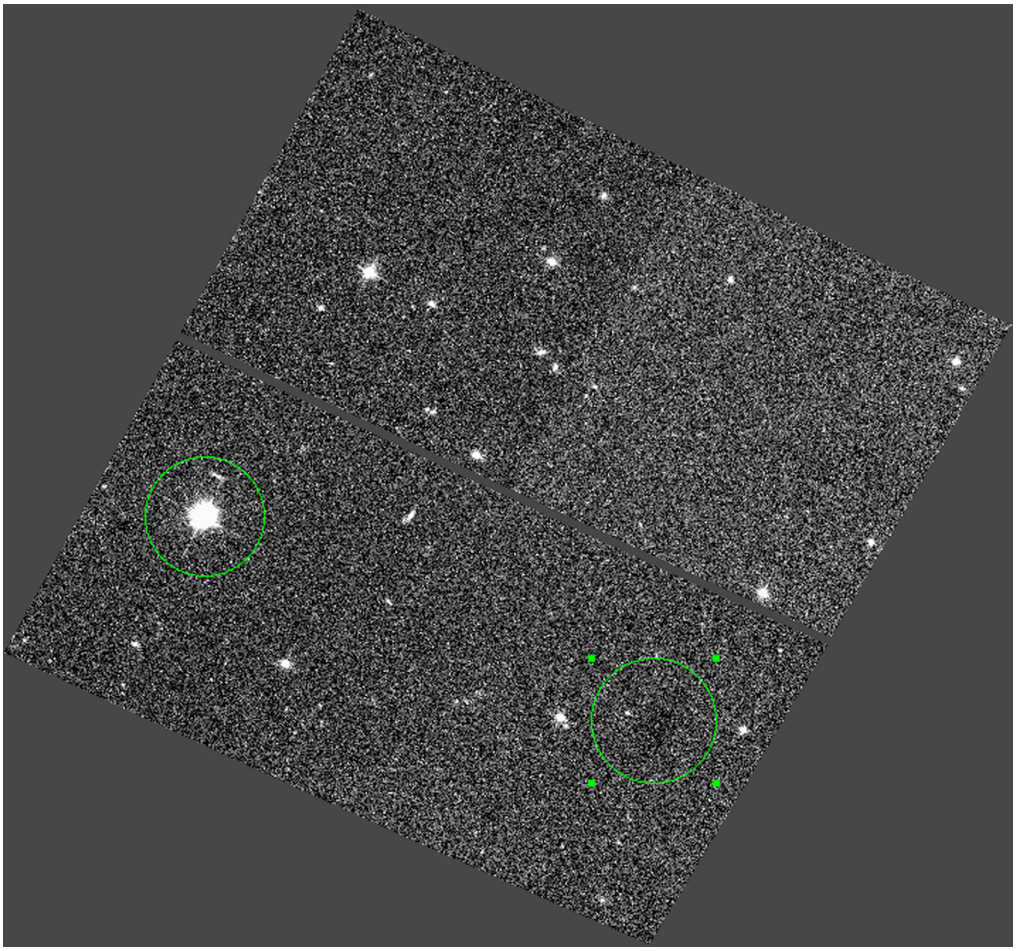

Figure 1.4 HST_9575_bm_ACS_WFC_F850LP_01_drz.fits shows a faint cross-talk image mirroring the star in the lower left quadrant.

1.5 Lamp Artifact

This major scattered light anomaly was a result of light from WFPC2 internal flats, taken at the same time as the ACS exposure, leaking into the ACS. Since the discovery of this anomaly in 2004, WFPC2 internal lamp observations are not scheduled during ACS exposures. A very small fraction of ACS science exposures were affected by this problem.

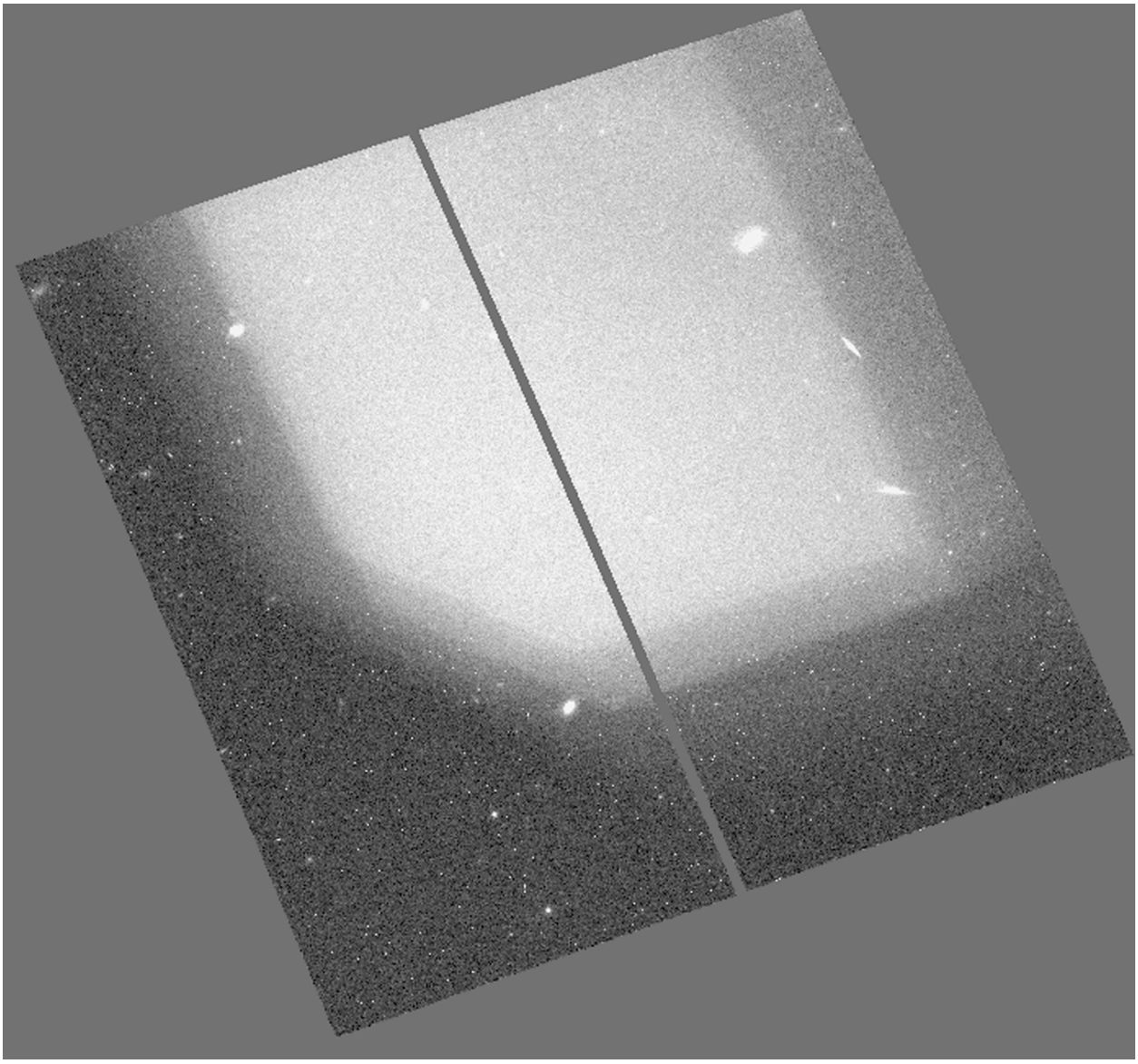

Figure 1.5 HST_9405_2t_ACS_WFC_F814W_01_drz.fits shows a large area illuminated by a light leak caused by WFPC2 internal lamps.

1.6 Telescope Guiding Loss of Lock on Guide Stars

Most HST observations are executed using Dual Guide Star mode, where two FGSs, each locked on a guide star, maintain a pointing accuracy of ~0.007" RMS over four orbits. In a Single Guide Star mode (used for short exposures and when one component of the Dual Guide Star mode fails), the telescope's translational motion is maintained by one FGS/guide star, while its roll is controlled by gyroscopes with a drift rate of 1.4 +/- 0.7 mas/sec. Rarely, complications can occur, as in the image below, obtained under gyro control, where the FGS was unable to lock on what turned out to be a bad guide star (double-star, since removed from the guide star catalog).

Additional Information:

Hubble Space Telescope Primer for Cycle 17, Sec. 3.2 HST Guiding Performance
http://www.stsci.edu/hst/proposing/documents/cp/Ch_3_TelescopePer3.html

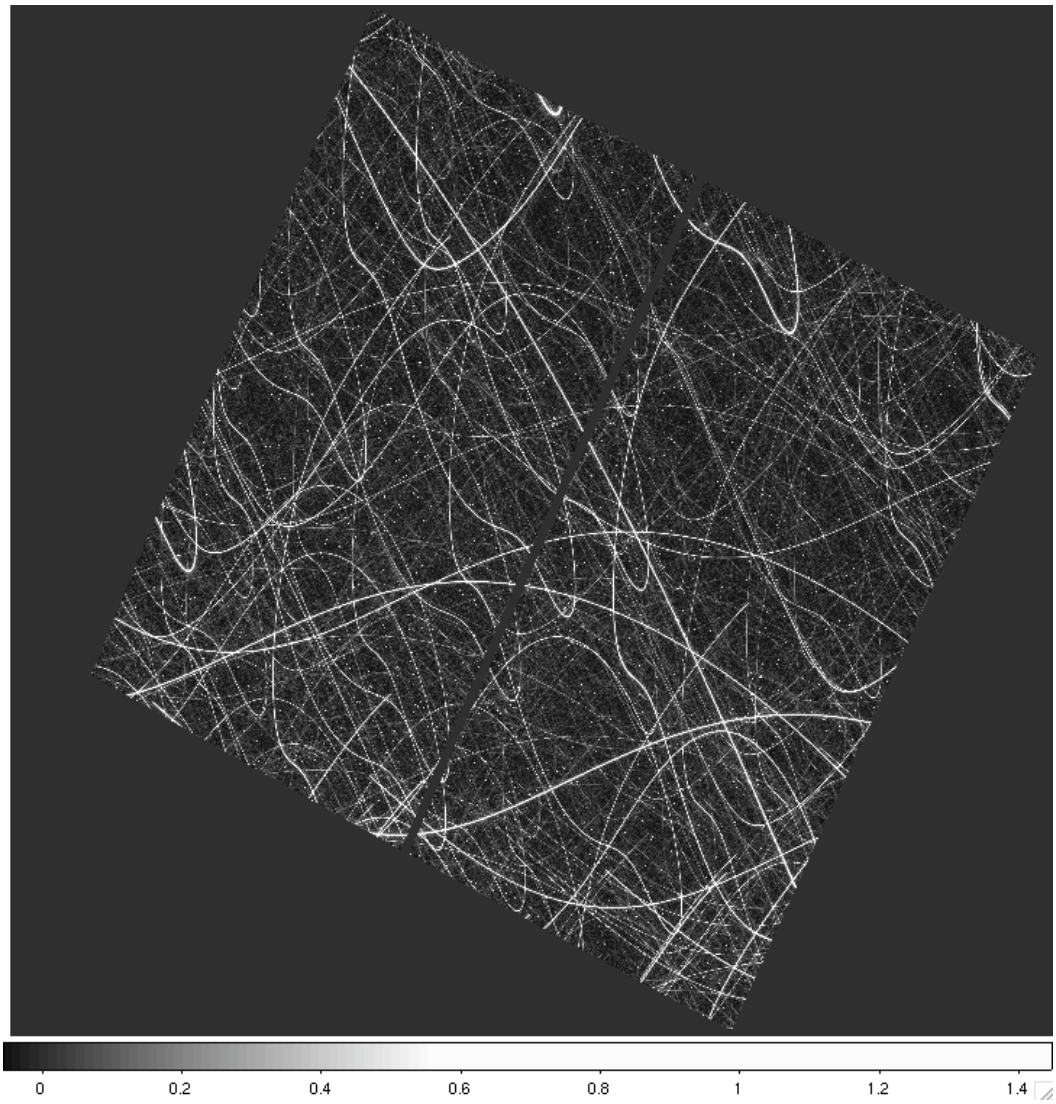

Figure 1.6 The long tangle of star trails in this image of NGC4833 (F814W, exposure time of 170s) was taken under gyroscope control because the FGS was unable to lock on a guide star.

2.0 Software-related Anomalies

2.1 Planetary Images not Aligned

Multidrizzle uses positions in the image header WCS to align drizzled images. However, this technique only works for fixed objects, not moving targets. There are plans for future enhancements to *multidrizzle* for dealing with moving targets, using target ephemeris data for image alignment. Until then, the images have to be manually aligned for use in *multidrizzle*. However, in most cases, single exposures are more scientifically useful for detecting motions of transient features on a planet or satellite.

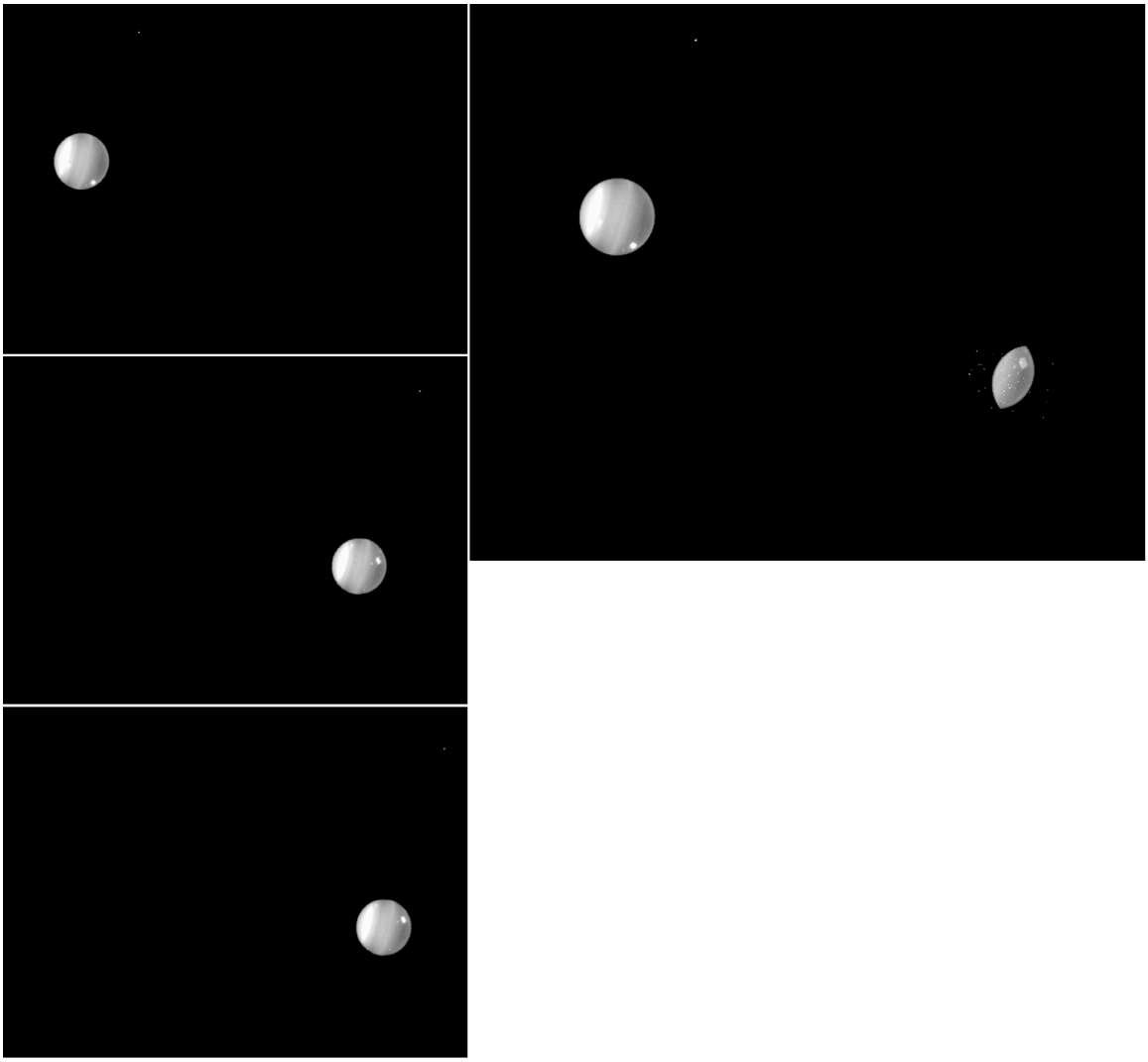

Figure 2.1 The images on the left are single exposures of Uranus. The multidrizzled image above, HST_10473_34_ACS_HRC_F814W_drz.fits, illustrates the typical problems associated with multidrzzled planetary images in the current pipeline.

2.2 Misaligned Images

Multidrizzle relies on the image header WCS to align dithered observations. But sometimes, WCS values can be slightly inaccurate, resulting in degraded Multidrizzle products due to misaligned images. For observations within an association, spanning over a few orbits and using the same guide star, thermal effects sometimes introduce misalignments as much as one pixel in the WFC, and two pixels in the HRC. In these cases, the image offsets have to be determined manually. A task called *tweakshifts*, in the *dither* package, has been developed for such scenarios, to allow users to determine shifts using cross-correlation or field object-matching.

HLA images are constructed automatically, therefore, there may be occasional misalignments. But most obvious cases have been recomputed so large misalignments should be rare.

Additional Information:

ACS Data Handbook, Section 4.6 Refining the Shifts: Manually and with Tweakshifts
http://www.stsci.edu/hst/acs/documents/handbooks/DataHandbookv5/ACS_longdhb.pdf

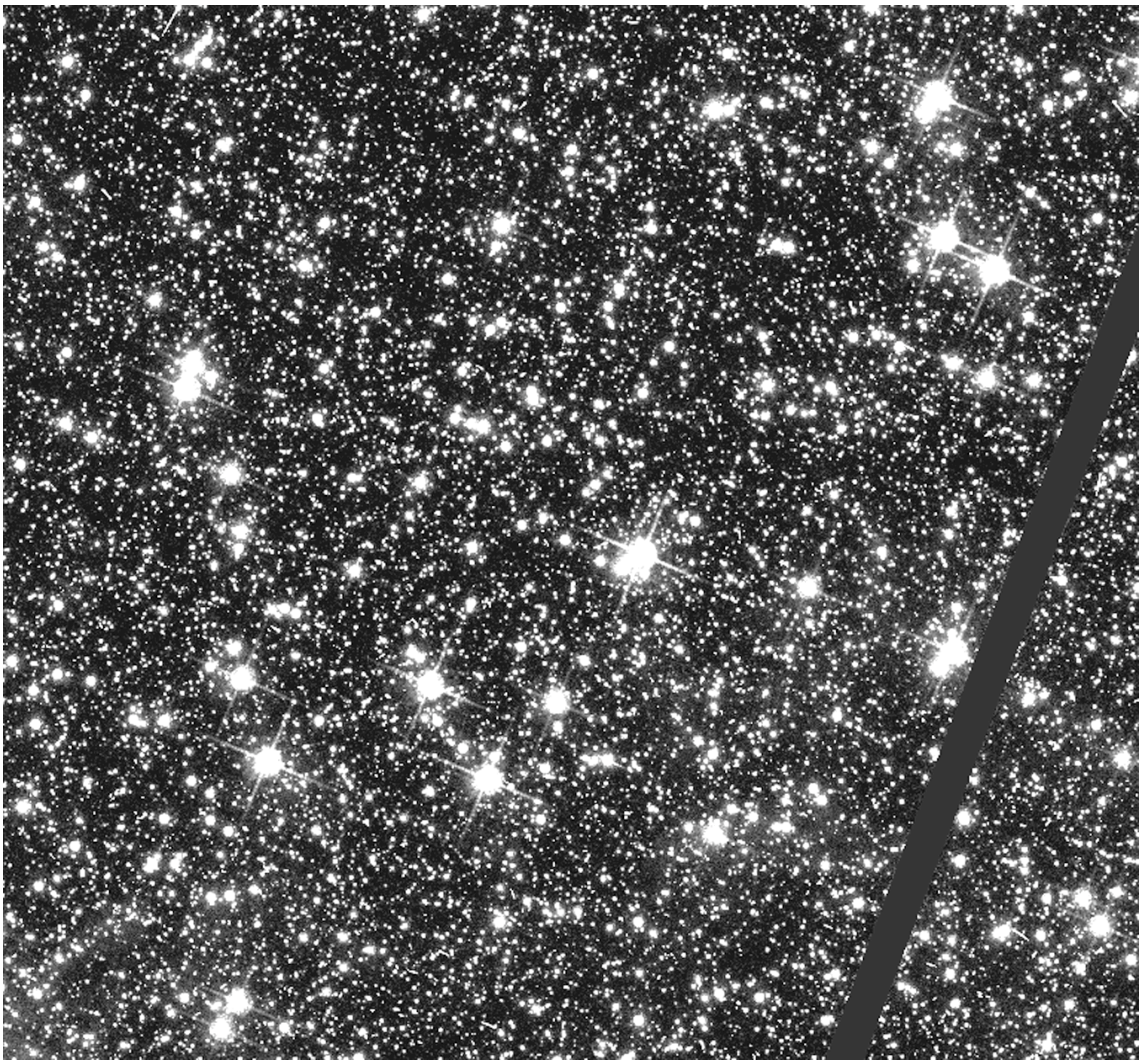

Figure 2.2a This is the first image (HST_9480_nx_ACS_WFC_F775W_01_drz.fits) in an association containing three exposures.

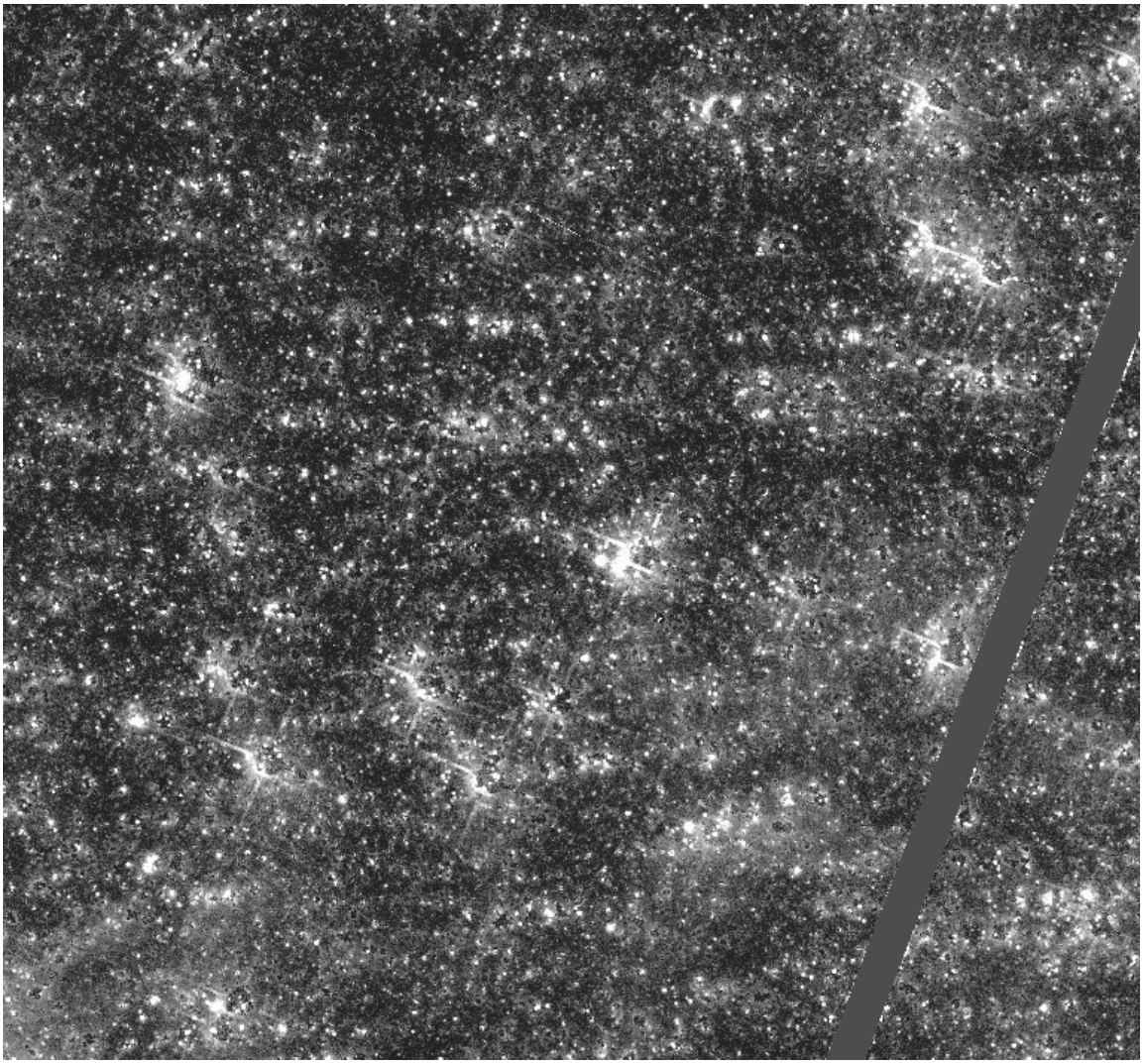

Figure 2.2b The second image, HST_9480_nx_ACS_WFC_F775W_drz.fits, is the combined image for that association, that was automatically processed by Multidrizzle. It clearly showed serious alignment problems before it was fixed.

2.3 “Bad” Color Combinations

The color images in the HLA database are created for cases where targets from the same proposal have been observed with different filters. The blue channel is assigned to images taken with the shortest wavelength passband, the red channel to the longest wavelength filter, and the green channel for a filter with wavelengths half-way between the two extremes. Therefore, blue is not necessarily assigned to blue filters, and red to red filters; i.e. these are not true color representations of the target. However, the color-combined images, as strange as some of them may look, are useful for highlighting interesting features visible in some filters and not others, hence the “bad” color combination images have been retained in the HLA.

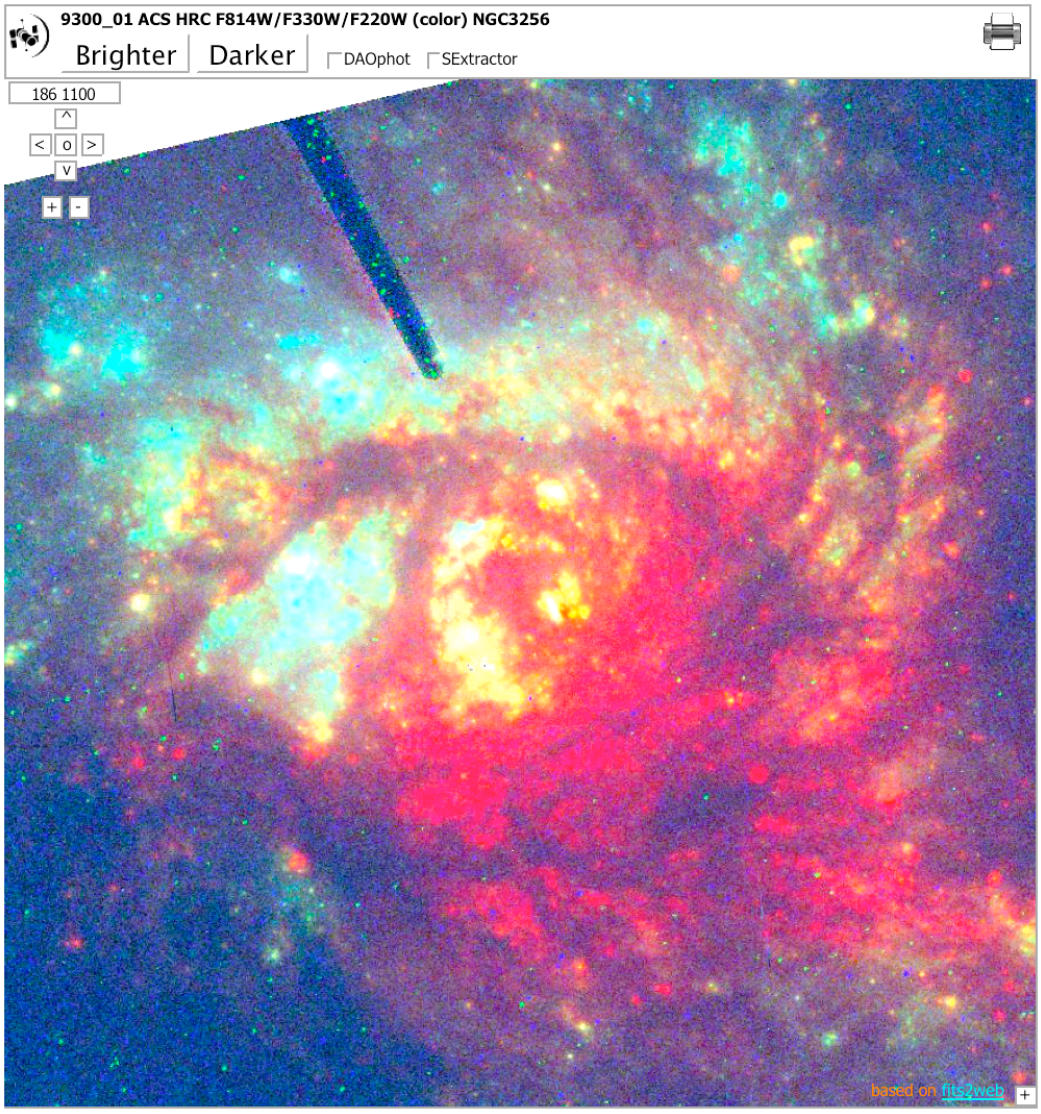

Figure 2.3 A color image of NGC3256, created from F814W (red channel), F330W (green), and F220W (blue) images. The dark rod at the top of the image is the HRC coronagraph finger.

2.4 Moiré Patterns, or Correlated Noise

Occasionally, an image combined by Multidrizzle will show faint background stripes or cross-hatched patterns. These features are more apparent in images with low signal-to-noise, such as a narrow-band filter image. Called Moiré patterns, or Correlated Noise, these interference patterns are artifacts created in a repixelated image when some sections of the pixel grid in one image are aligned with pixels in the original image (hence retaining the full RMS noise), while other sections of the pixel grid line up between pixels of the original image (leading to an interpolation that smoothes the image and reduces the RMS noise). This happens, for example, when significant geometric corrections are applied to the images. It can also result from drizzling individual input images that have a different grid size from the combined image (for example, by setting *multidrizzle.final_pixfra* to a value less than 1).

Additional Information:

Wikipedia entry for Moiré pattern

http://en.wikipedia.org/wiki/Moiré_pattern

Correlated Noise in ACS Drizzled Images (Q&A from STScI ACS Forum)

http://forums.stsci.edu/phpbb/viewtopic.php?p=175

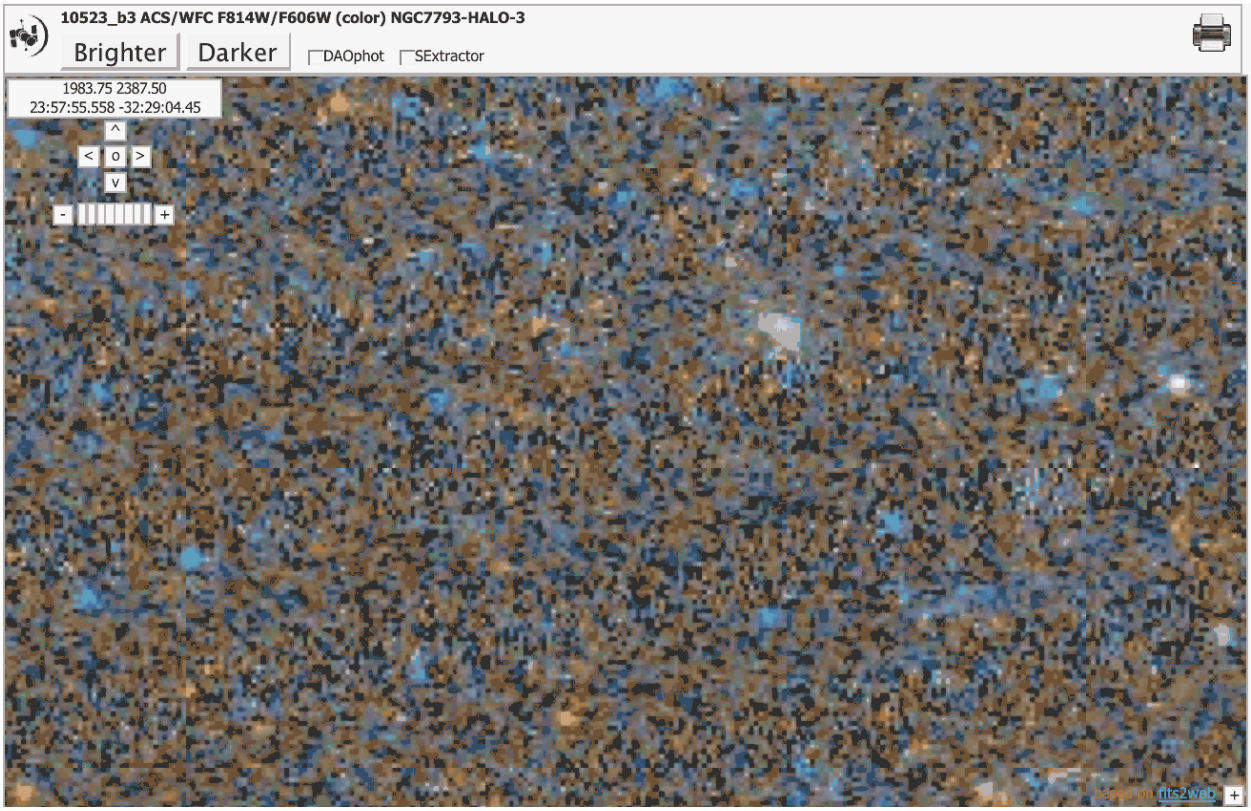

Figure 2.4 This is a close-up of the background in image 10523_b3_ACS_WFC_F814W_F606W. Usually, correlated noise is a very low-level effect. In this image, we have stretched the contrast very hard to make it visible. Moiré noise can also be seen in Figure 4.5a, which is a close-up section of the WFC illuminated by scattered light.

2.5 Image Compression Anomaly

The partial herringbone pattern seen in this WFC image is caused by the compression of one quadrant in the image. The data from one of the four amplifiers was compressed to allow the storage of a HRC image taken in parallel with the primary WFC observation. The data compression and subsequent decompression corrupted portions of that image quadrant, producing the anomalous signature. This anomaly is very rare in science images because compression is usually disabled for external observations. During the first years of ACS operation, internal bias and dark frames were compressed and a similar feature was present in those single images, although at a much lower level and in all four quadrants.

Additional information:

ACS ISR 2004-07 Bias and Dark Calibration of ACS Data

http://www.stsci.edu/hst/acs/documents/isrs/isr0407.pdf

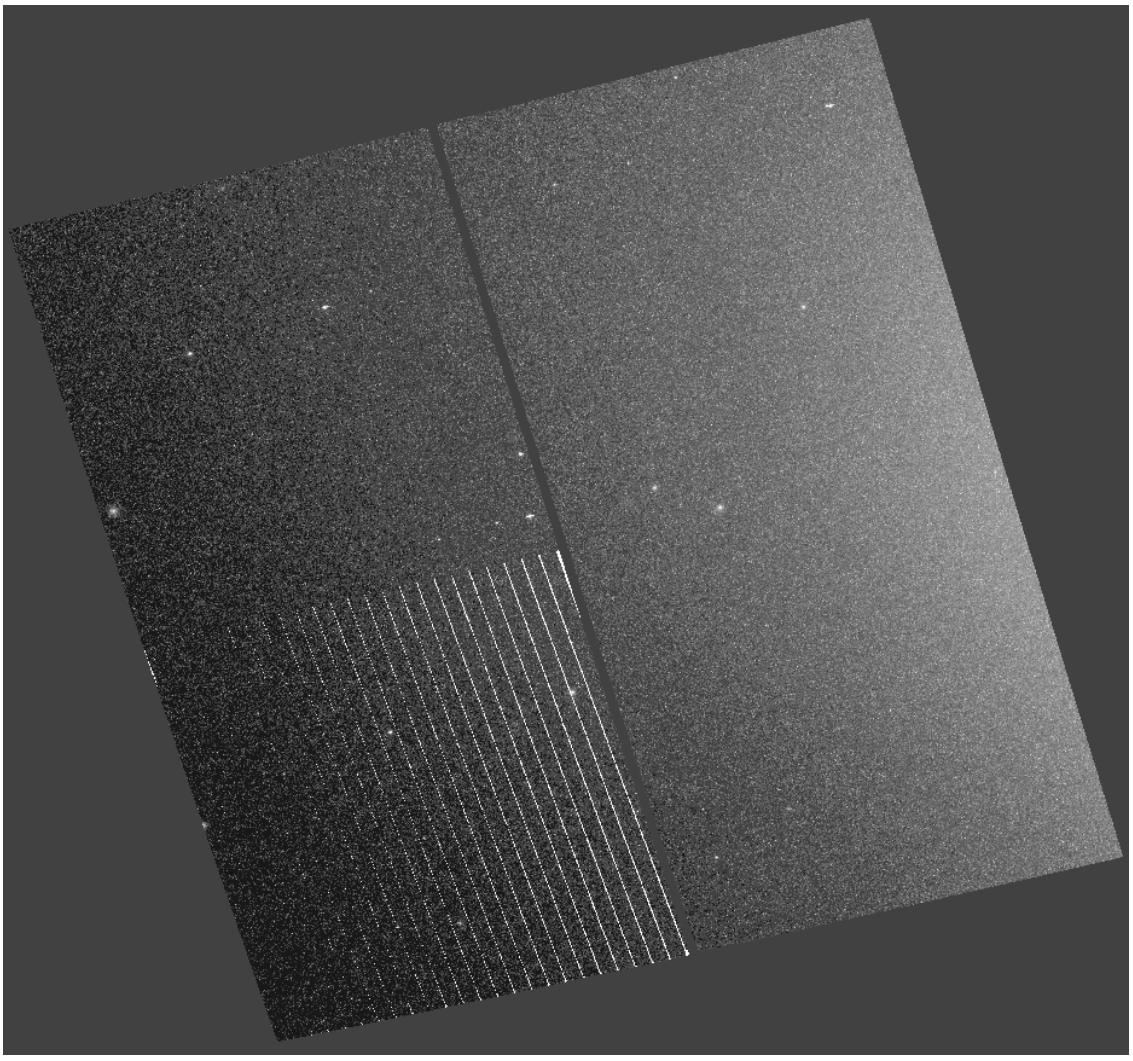

Figure 2.5 Image HST_10118_05_ACS_WFC_F814W_drz.fits is an example of the anomaly described above. Twenty-four individual images were drizzled to create this image, and each had the same-features in the same quadrant.

2.6 Data Dropouts

Data dropouts, where a portion of the image appears blank, sometimes occurs due to processing problems. These can usually be fixed, so please contact *archive@stsci.edu* if you notice a problem.

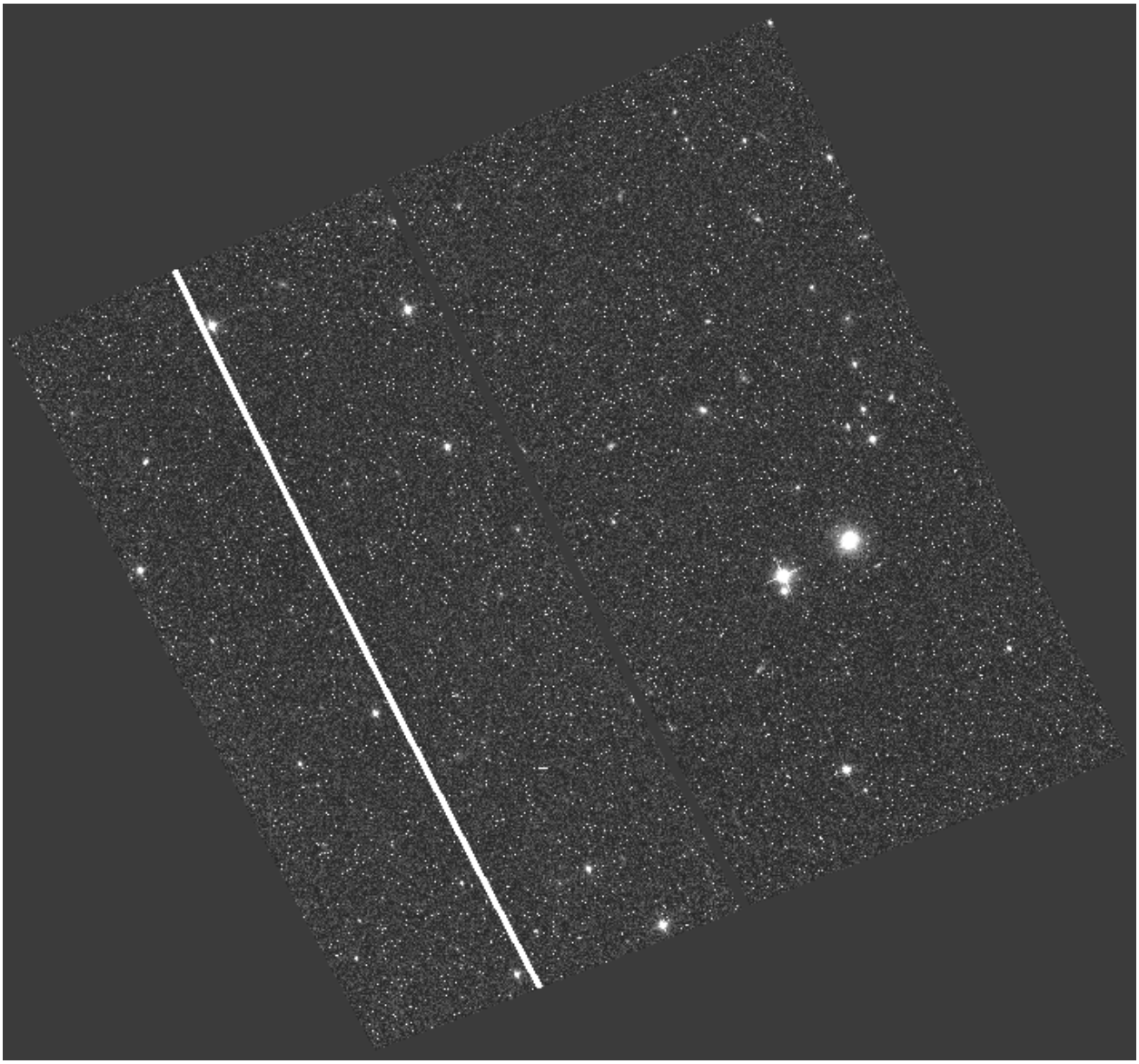

Figure 2.6 HST_9482_al_ACS_WFC_F850LP_drz.fits shows a data dropoff due to a processing error. Typically, these anomalies can easily be fixed.

3.0 Moving target features

3.1 Asteroid Trail

Occasionally, a short streak, not caused by cosmic rays, is seen in ACS images of fixed targets. These are trails from asteroids passing through the field-of-view during the exposure.

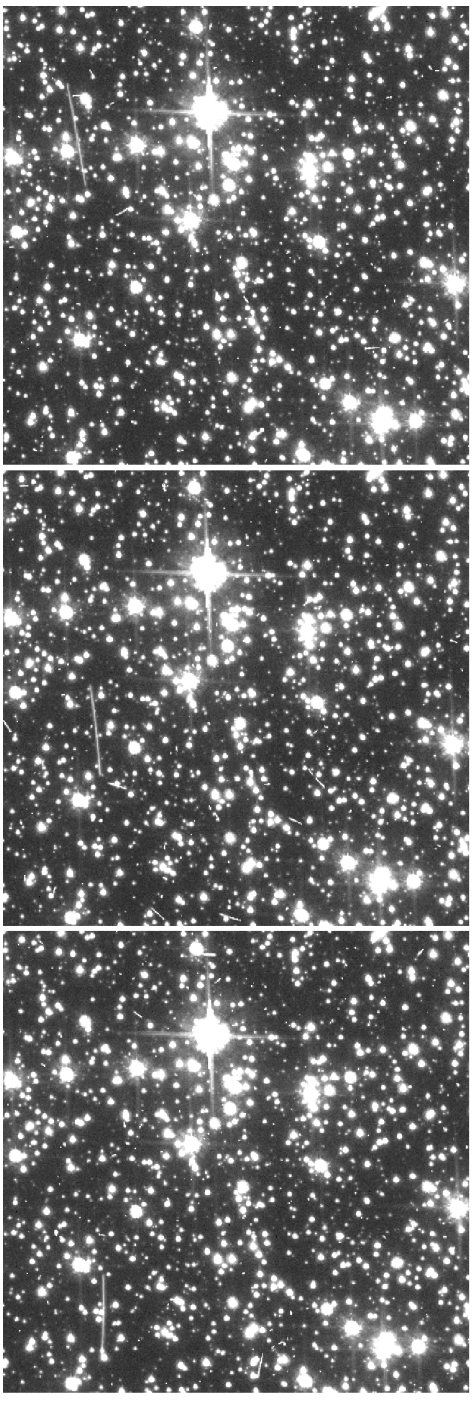

Figure 3.1 An asteroid trail in three consecutive WFC images. Data from the SWEEPS (Sagittarius Window Eclipsing Extrasolar Planet Search) survey, GO proposal 9750, courtesy of Kailash Sahu, STScI.

3.2 Satellite trail

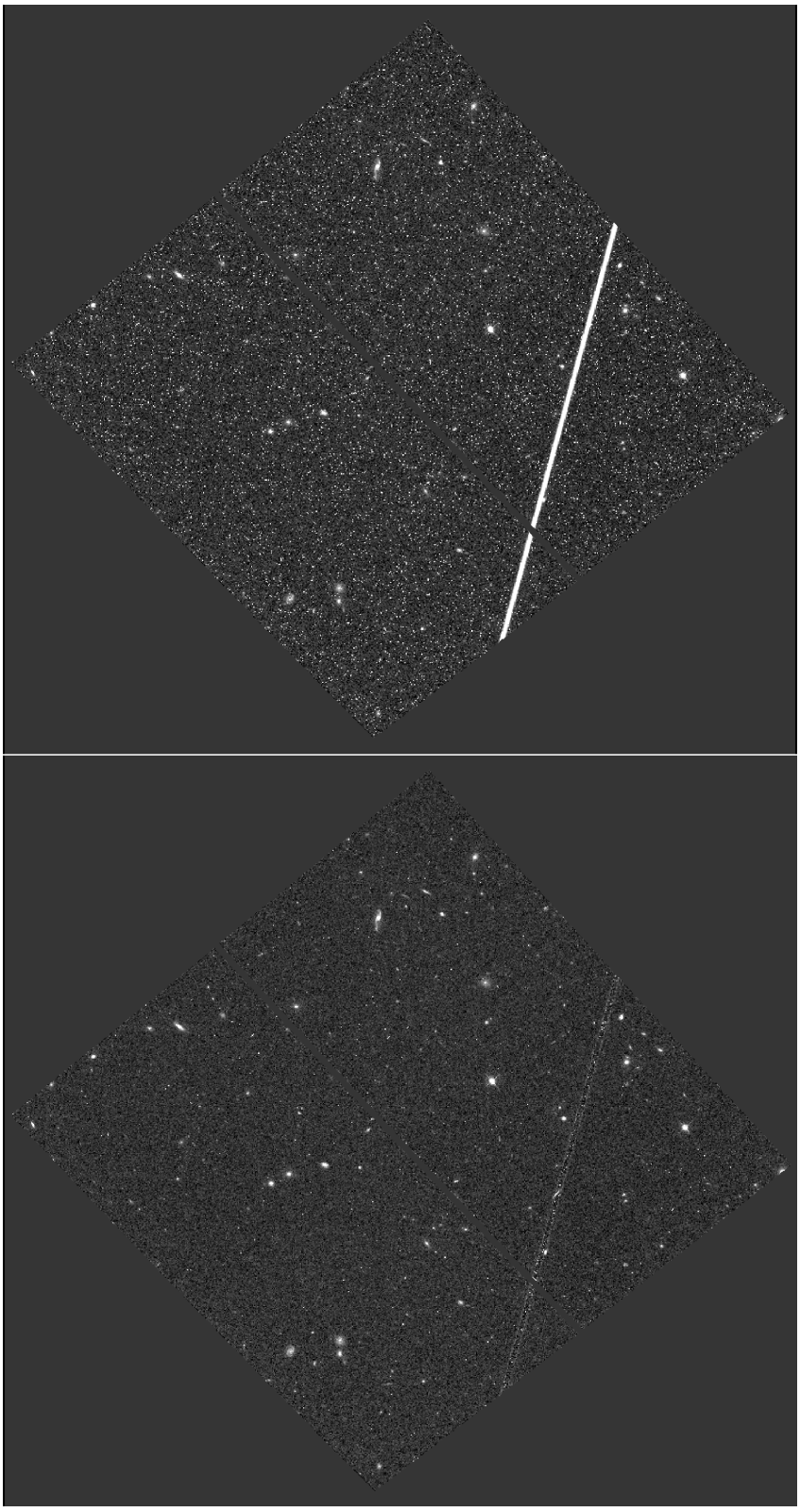

Satellites passing across the field-of-view during an exposure leave a long trail across the image. These can be removed if the affected image is part of a suitable dither set.

Figure 3.2 The top image is an individual image (HST_9075_1e_ACS_WFC_F850LP_02_drz.fits) with a satellite trail. It was part of a CR-SPLIT pair of images at the same pointing. There was no satellite trail in the other individual image. When the two images were combined in Multidrizzle, the trail artifact was removed; however a faint residual can be seen in the combined image shown below, HST_9075_1e_ACS_WFC_F850LP_drz.fits

4.0 Optical Anomalies

4.1 Dragon's Breath

Dragon's Breath is a shower of scattered light from a very bright star that is just off the edge of the CCD. This rare anomaly occurs when a star falls at the edge of the mask in front of the chip; the starlight reflects off the CCD, then off the mask, and back to the detector.

Additional Information:

ACS Data Handbook, Section 5.5.2 Optical Ghosts and Scattered Light
http://www.stsci.edu/hst/acs/documents/handbooks/DataHandbookv5/ACS_longdhb.pdf

On-orbit alignment and imaging performance of the HST Advanced Camera for Surveys, G.F. Hartig, et. al.
http://www.stsci.edu/hst/acs/performance/anomalies/ACS_ghosts.pdf

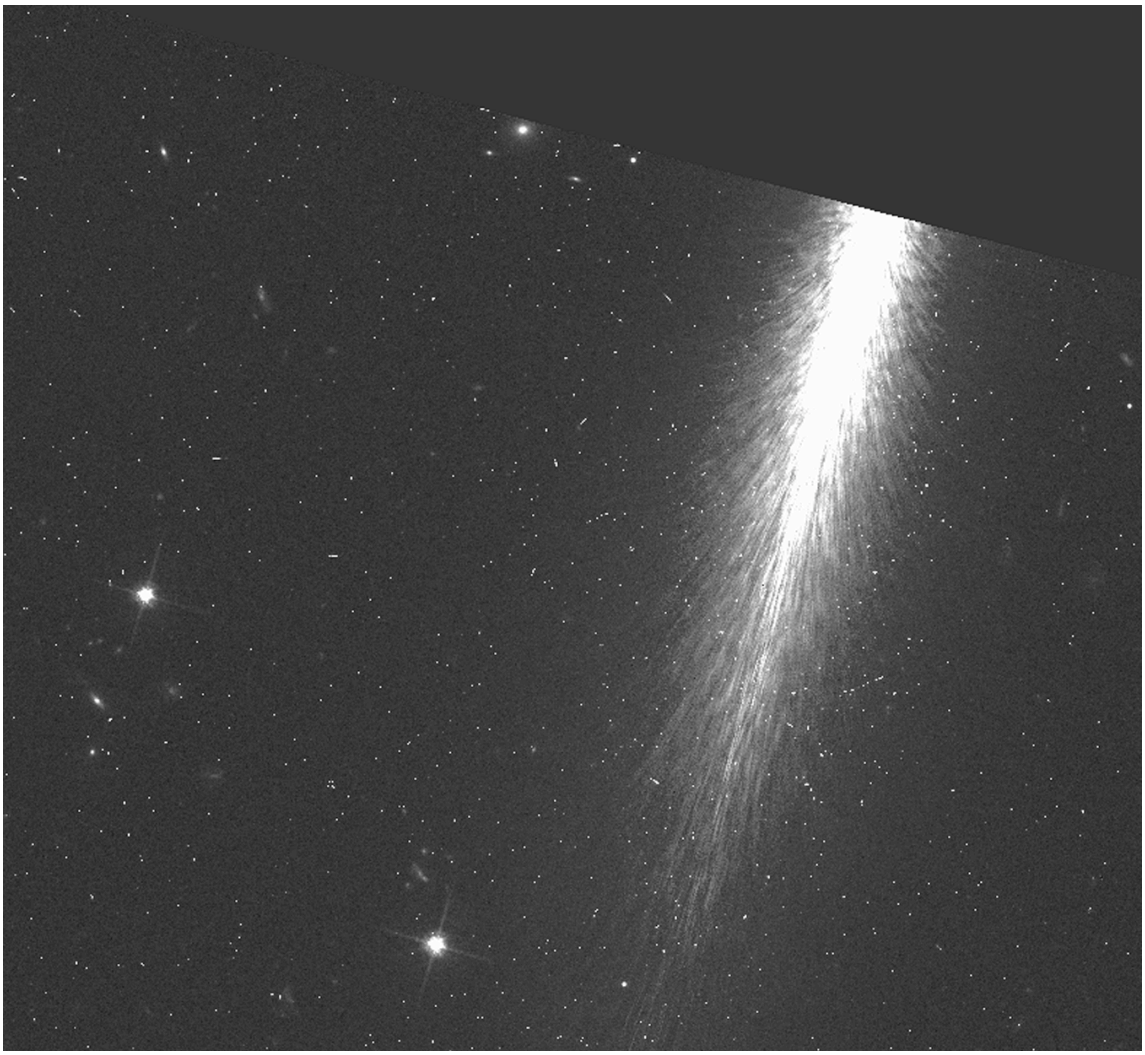

Figure 4.1 Dragon's Breath feature in HST_9033_01_ACS_WFC_F814W_01_drz.fits

4.2 Filter Ghosts

Some filters, especially narrow-band filters such as F660N, have internal reflections that produce pairs of fairly bright circular annuli, extending out radially near the target. These haloes, about 10 to 20 pixels in diameter, are about 2% of the target's energy.

Additional Information:

ACS Data Handbook, Section 5.5.2 Optical Ghosts and Scattered Light
http://www.stsci.edu/hst/acs/documents/handbooks/DataHandbookv5/ACS_longdhb.pdf

On-orbit alignment and imaging performance of the HST Advanced Camera for Surveys, G.F. Hartig, et. al.
http://www.stsci.edu/hst/acs/performance/anomalies/ACS_ghosts.pdf

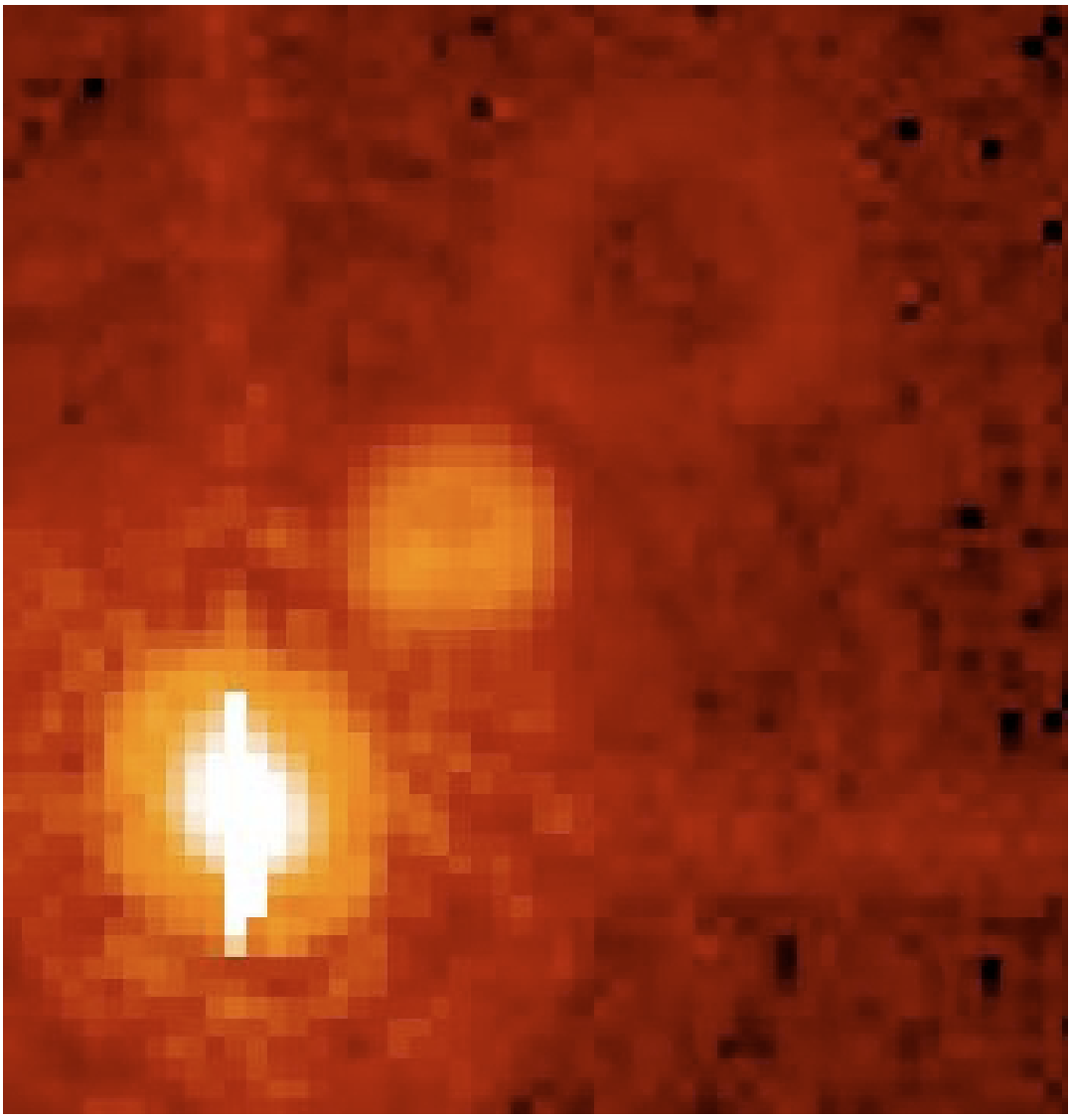

Figure 4.2 The F660N filter ghost, image from the Hartig et. al. paper mentioned above.

4.3 Optical Ghosts

There are three kinds of annular optical ghosts which are usually visible when there is a bright star, or several bright stars in the field:

1. **Pairs of elliptical rings**: bright targets in the WFC's lower right quadrant (D-amplifier) create reflections resembling a pair of elliptical rings, like the number 8. The positions of these features depends on the location of the offending source in quadrant D. Also, reflections closer to the quadrant corner are brighter and larger. The rings are created by reflections from the CCD surface (which lies at ~20° to the chief ray), up to the detector windows, then back to the CCD.
2. **Large annular ghosts**: caused by reflection from the detector window, to the filters, and back to the CCD,and are seen near bright objects.
3. **Small annular feature**: created by reflections between the inner and outer window surfaces; These are smaller and fainter, and found much closer to the parent object.

Additional Information:

ACS Data Handbook, Section 5.5.2 Optical Ghosts and Scattered Light
http://www.stsci.edu/hst/acs/documents/handbooks/DataHandbookv5/ACS_longdhb.pdf

On-orbit alignment and imaging performance of the HST Advanced Camera for Surveys, G.F. Hartig, et. al.
http://www.stsci.edu/hst/acs/performance/anomalies/ACS_ghosts.pdf

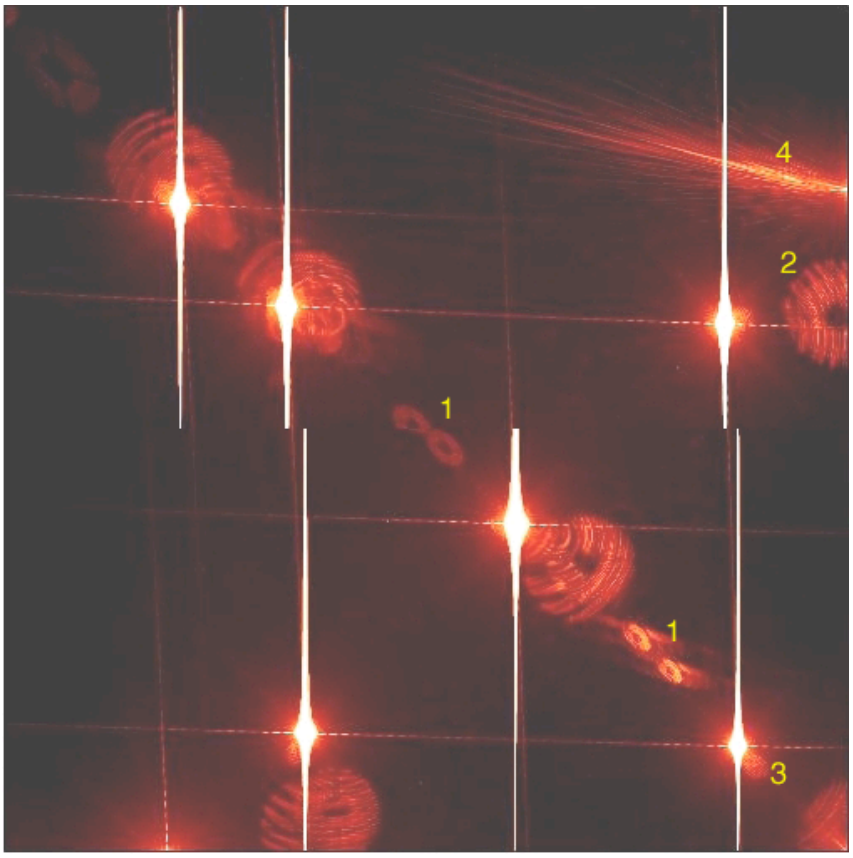

Figure 4.3a This image taken during ACS thermal vac ground testing (Hartig et. al), shows four types of optical reflections.

1. Elliptical ring pairs.
2. Large Annulus.
3. Small Annulus
4. Dragon's breath

Feature #2 can also be seen in Figure 1.2.

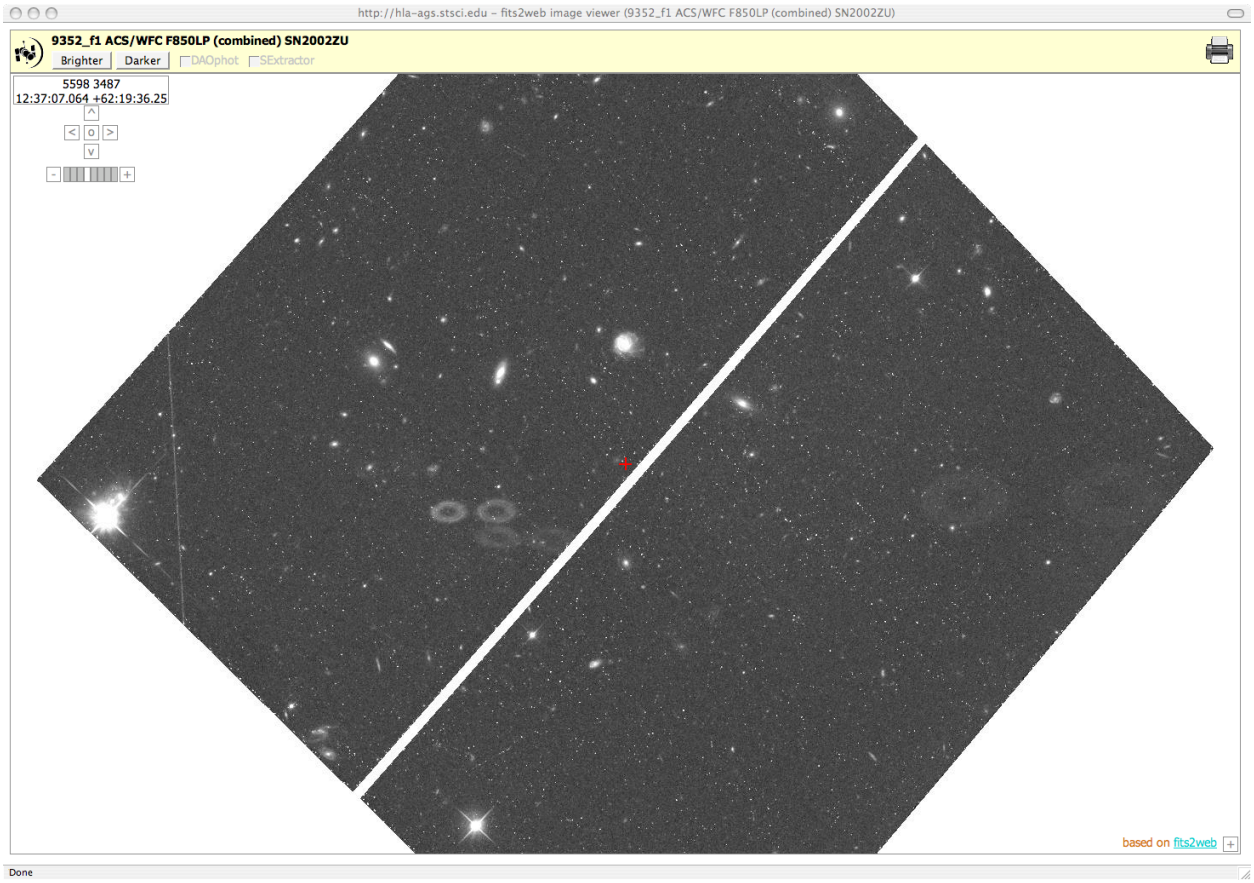

Figure 4.3b In this image, HST_9352_f1_ACS_WFC_F850LP_drz.fits, a pair of double elliptical rings are visible left of the image center. At the extreme right of the image, two much fainter elliptical rings are visible. These reflections are a result of the bright star in in quadrant D (left corner of the image).

4.4 Glint

A star that falls in the gap between the two WFC CCDs can sometimes create a reflection known as a “glint”, thin rays of light extending from the chip gap. These rays are the reflection of starlight off the residual indium solder used for chip attachment.

Additional Information:

ACS Data Handbook, Section 5.5.2 Optical Ghosts and Scattered Light
http://www.stsci.edu/hst/acs/documents/handbooks/DataHandbookv5/ACS_longdhb.pdf

On-orbit alignment and imaging performance of the HST Advanced Camera for Surveys, G.F. Hartig, et. al.
http://www.stsci.edu/hst/acs/performance/anomalies/ACS_ghosts.pdf

Scatter from the ACS WFC Inter-chip Gap, George Hartig, 2002
http://www.stsci.edu/hst/acs/performance/anomalies/ACS_scatter.pdf

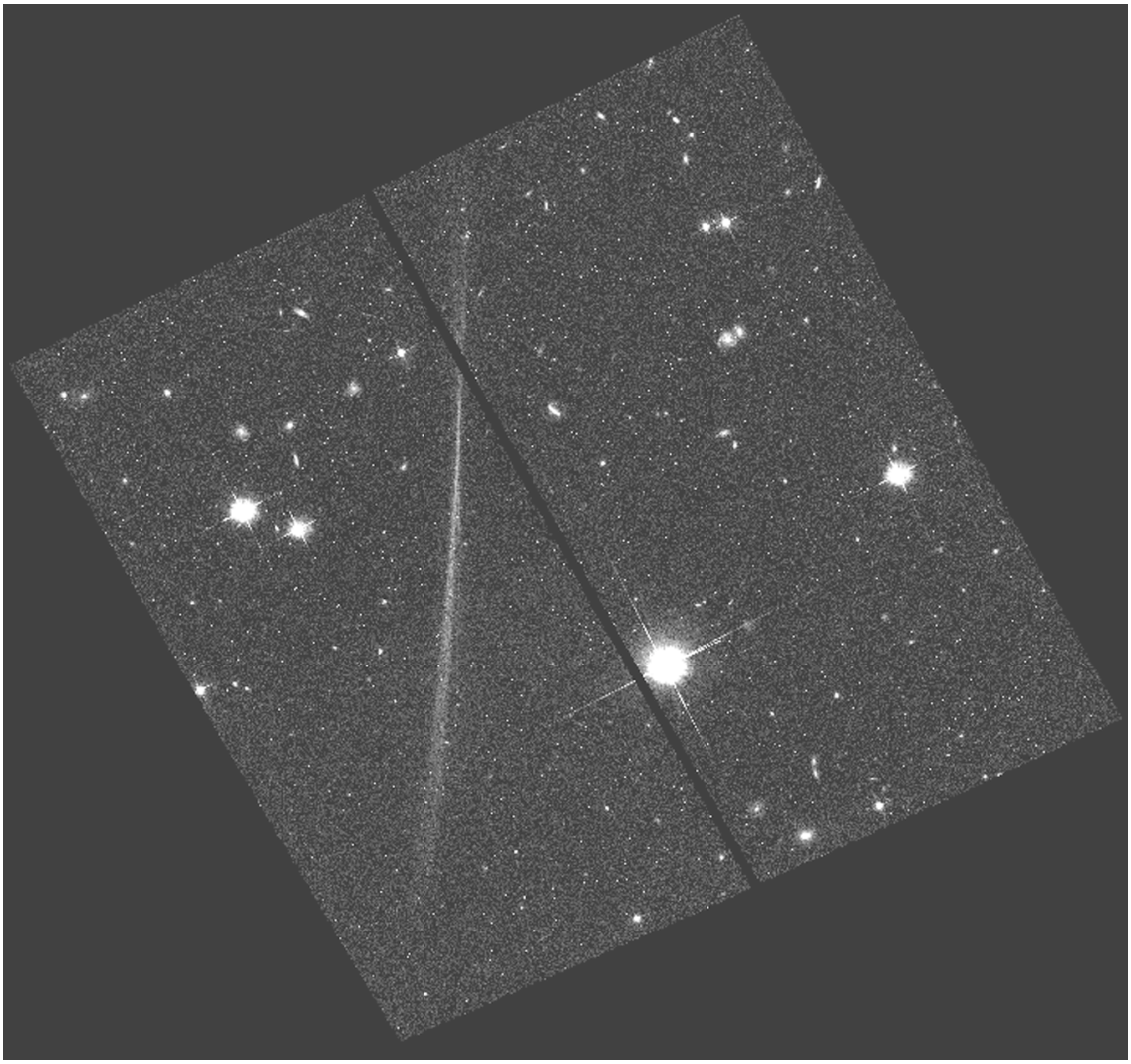

Figure 4.4 A reflection feature created by a star located at the chip gap, in image HST_9468_9k_ACS_WFC_F814W_01_drz.fits

4.5 Dust Rings and Scattered Earth Light

Circular patterns (dark rings with bright centers), seen in ACS flat fields, are created by dust on the CCD windows. Similar but larger features are created by dust on filters. For almost all calibrated images, dust patterns are removed during flat-fielding. However, the dust rings appear more prominent if scattered light reaches the detector. Scattered light due to the bright Earth limb is a rare occurrence because observations are never taken when the bright Earth avoidance angle is less than 20°.

However, on rare occasions, when observing targets in the Continuous Viewing Zone (within 24° of orbital poles), scattered Earth light is able to intrude into an exposure, causing dust features to appear in an image. This would happen if the Sun's altitude is just a few degrees below the Earth's horizon, but sunlight scattered by the Earth's atmosphere manages to illuminate the camera, causing a brighter background in the image. A thin sliver of scattered sunlight just before sunrise is well-collimated, compared to a fully-illuminated bright Earth, and will cast distinctive shadows of the dust particles, creating dark rings with bright centers, as seen in Figures 4.5a & b.

Additional Information:

ACS Data Handbook, Section 5.5.1 Dust Motes

ACS Data Handbook, Section 5.5.4 Scattered Earth Light

http://www.stsci.edu/hst/acs/documents/handbooks/DataHandbookv5/ACS_longdhb.pdf

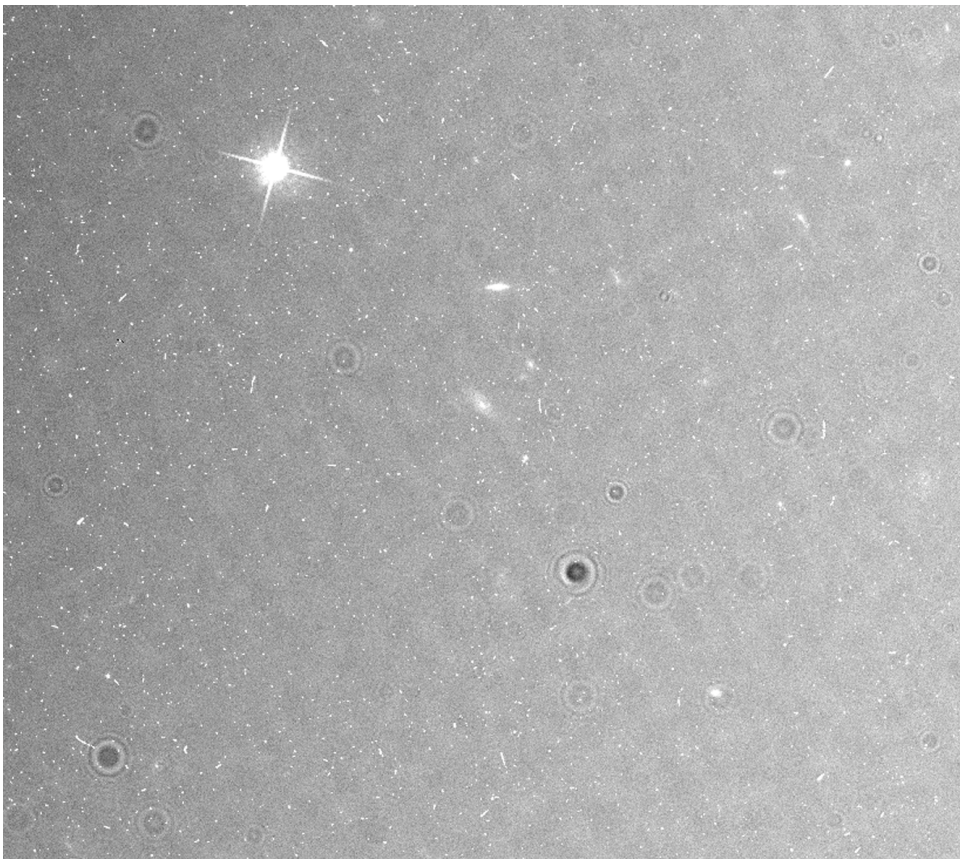

Figure 4.5a Close-up of dust rings in HST_9468_a8_ACS_WFC_F814W_drz.fits. In this example, the target declination was 62°. At the time of the exposure, the sun altitude was -2°, just below the Earth horizon. Although the observation was executed while the telescope was in Earth shadow, some sunlight, scattered by the Earth's atmosphere, was able to illuminate the camera, casting deep shadows of dust particles on the CCD windows and filters.

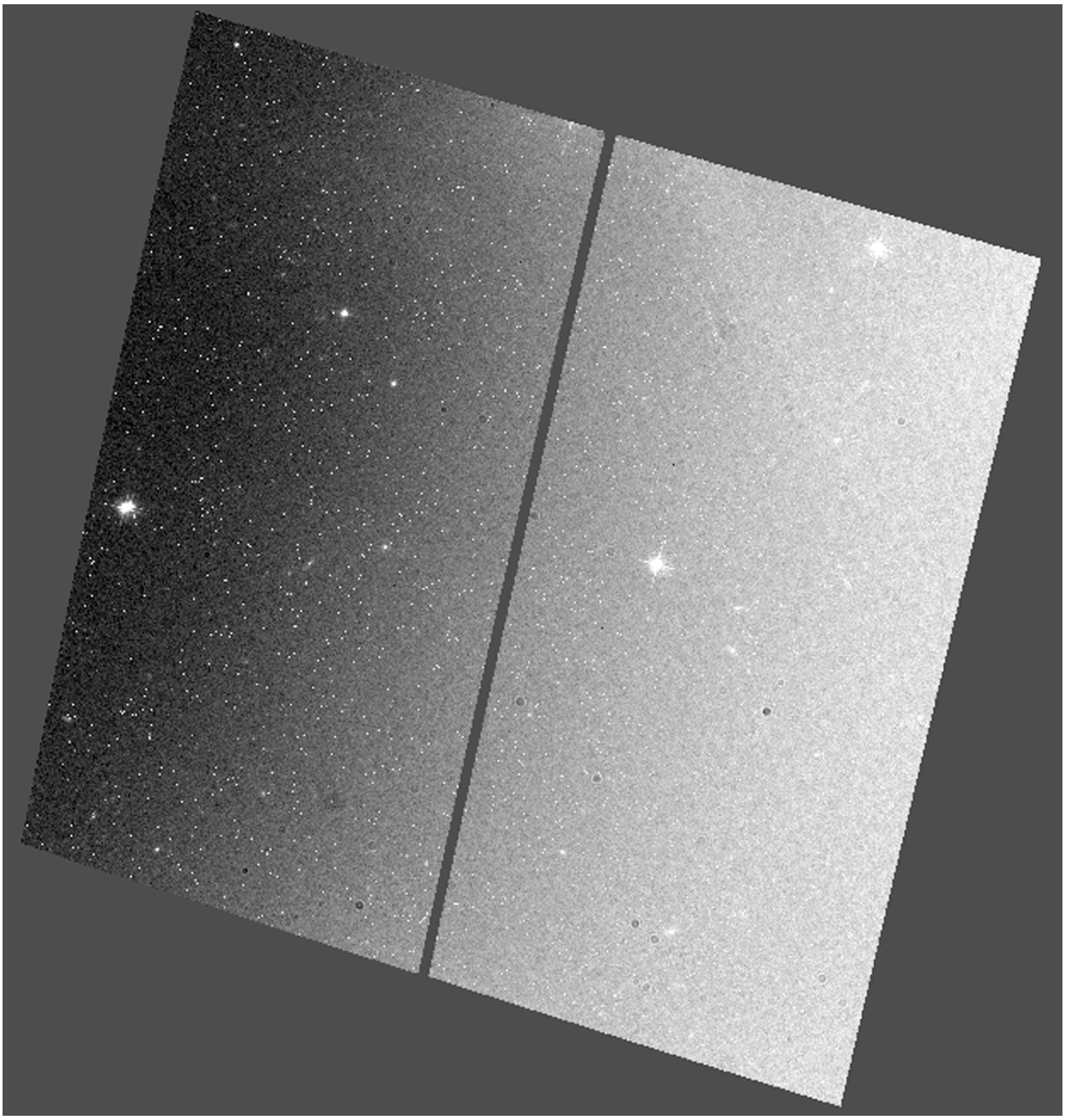

Figure 4.5b Image HST_9468_a8_ACS_WFC_F814W_drz.fits, showing a light gradient due to scattered light just before sunrise in HST orbit.

Acknowledgments

Special thanks to Marco Sirianni and Ron Gilliland for reviewing this ISR. We are grateful for the work by members of the HLA and ACS teams, who laid the foundations that made this ISR possible.

References

ACS Anomalies and Artifacts
http://www.stsci.edu/hst/acs/performance/anomalies

ACS Instrument Handbook, Section 5.5 Image Anomalies
http://www.stsci.edu/hst/acs/documents/handbooks/DataHandbookv5/acs_Ch56.html#95178

On-orbit alignment and imaging performance of the HST Advanced Camera for Surveys
G.F. Hartig, et. al 2002
http://www.stsci.edu/hst/acs/performance/anomalies/ACS_ghosts.pdf

Scatter from the ACS WFC Inter-chip Gap
G. F. Hartig 2002
http://www.stsci.edu/hst/acs/performance/anomalies/ACS_scatter.pdf

ACS Instrument Handbook, v. 7.1
Pavlovsky, C., et al. 2006
http://www.stsci.edu/hst/acs/documents/handbooks/cycle16/cover.html

ACS Data Handbook, v.5.0
Pavlovsky, C., et al. 2006
http://www.stsci.edu/hst/acs/documents/handbooks/DataHandbookv5/ACS_longdhbcover.html

Bias Subtraction and Correction of ACS/WFC Frames
Sirianni et al. 2002
http://www.stsci.edu/hst/HST_overview/documents/calworkshop/workshop2002/CW2002_Papers/CW02_sirianni

ACS data quality flags
http://www.stsci.edu/hst/acs/analysis/reference_files/data_quality_flags.html

ISR 95-06: A Field Guide to WFPC2 Image Anomalies
Biretta, et. al. 1995
http://www.stsci.edu/hst/wfpc2/analysis/wfpc2_anomalies.html